

# Transgenic Mice Overexpressing Mutant *PRKAG2* Define the Cause of Wolff-Parkinson-White Syndrome in Glycogen Storage Cardiomyopathy

Michael Arad, MD; Ivan P. Moskowitz, MD, PhD; Vickas V. Patel, MD, PhD; Ferhaan Ahmad, MD, PhD; Antonio R. Perez-Atayde, MD; Douglas B. Sawyer, MD, PhD; Mark Walter, BS; Guo H. Li, MD; Patrick G. Burgon, MD, PhD; Colin T. Maguire, BS; David Stapleton, PhD; Joachim P. Schmitt, MD; X.X. Guo, BS; Anne Pizard, PhD; Sabina Kupersmidt, MD; Dan M. Roden, MD; Charles I. Berul, MD; Christine E. Seidman, MD; J.G. Seidman, PhD

**Background**—Mutations in the  $\gamma_2$  subunit (*PRKAG2*) of AMP-activated protein kinase produce an unusual human cardiomyopathy characterized by ventricular hypertrophy and electrophysiological abnormalities: Wolff-Parkinson-White syndrome (WPW) and progressive degenerative conduction system disease. Pathological examinations of affected human hearts reveal vacuoles containing amylopectin, a glycogen-related substance.

**Methods and Results**—To elucidate the mechanism by which *PRKAG2* mutations produce hypertrophy with electrophysiological abnormalities, we constructed transgenic mice overexpressing the *PRKAG2* cDNA with or without a missense N488I human mutation. Transgenic mutant mice showed elevated AMP-activated protein kinase activity, accumulated large amounts of cardiac glycogen (30-fold above normal), developed dramatic left ventricular hypertrophy, and exhibited ventricular preexcitation and sinus node dysfunction. Electrophysiological testing demonstrated alternative atrioventricular conduction pathways consistent with WPW. Cardiac histopathology revealed that the annulus fibrosus, which normally insulates the ventricles from inappropriate excitation by the atria, was disrupted by glycogen-filled myocytes. These anomalous microscopic atrioventricular connections, rather than morphologically distinct bypass tracts, appeared to provide the anatomic substrate for ventricular preexcitation.

**Conclusions**—Our data establish *PRKAG2* mutations as a glycogen storage cardiomyopathy, provide an anatomic explanation for electrophysiological findings, and implicate disruption of the annulus fibrosus by glycogen-engorged myocytes as the cause of preexcitation in Pompe, Danon, and other glycogen storage diseases. (*Circulation*. 2003;107:2850-2856.)

**Key Words:** kinases ■ glycogen storage disease ■ excitation ■ arrhythmia ■ hypertrophy

Human mutations in *PRKAG2*, the gene encoding the  $\gamma_2$  subunit of AMP-activated protein kinase (AMPK), cause cardiomyopathy characterized by ventricular hypertrophy, Wolff-Parkinson-White syndrome (WPW), and progressive conduction system disease.<sup>1-5</sup> AMPK, consisting of catalytic ( $\alpha$ ) and regulatory ( $\gamma$  and  $\beta$ ) subunits, is activated in energy-deficiency states and plays a key role in regulation of cardiac metabolism and energy homeostasis.<sup>1</sup> In vitro analyses of the biochemical consequences of disease-causing missense mutations in a yeast gene homologue (*Snf4*) and in transfected COS cells indicated that defects in humans caused

constitutive kinase activity.<sup>5,6</sup> We have documented vacuolar changes and periodic acid-Schiff (PAS)-positive inclusions, suggesting accumulation of glycogen-related material, in the hearts of affected individuals.<sup>5</sup> Although they clearly distinguish this entity from classic hypertrophic cardiomyopathy caused by sarcomere protein gene mutation,<sup>7</sup> the exact role played by glycogen stores in disease pathogenesis remains unclear.

An intriguing and poorly understood aspect of this disorder is the conduction system disease associated with *PRKAG2* mutations. Affected individuals typically demonstrate ECG

Received December 23, 2002; revision received March 4, 2003; accepted March 5, 2003.

From the Department of Genetics, Harvard Medical School and Howard Hughes Medical Institute (M.A., I.P.M., F.A., G.H.L., P.G.B., J.P.S., A.P., C.E.S., J.G.S.), the Department of Pathology and Cardiac Registry, Children's Hospital, and Harvard Medical School (I.P.M., A.R.P.-A.), the Department of Cardiology, Children's Hospital and Department of Pediatrics, Harvard Medical School (V.V.P., C.T.M., C.I.B.), Boston University Medical Center, Myocardial Biology Unit (D.B.S., X.X.G.), and the Division of Cardiology, Brigham and Women's Hospital (C.E.S.), Boston, Mass; the Molecular Cardiology Research Center and Section of Cardiac Electrophysiology, University of Pennsylvania, Philadelphia (V.V.P.); St Vincent's Institute of Medical Research, Victoria, Australia (M.W., D.S.); and the Departments of Anesthesiology and Pharmacology (S.K.) and Medicine, Pharmacology, Molecular Physiology, and Biophysics (D.M.R.), Vanderbilt University School of Medicine, Nashville, Tenn.

Correspondence to Jonathan Seidman, PhD, Department of Genetics, Alpert Room 533, Harvard Medical School, 200 Longwood Ave, Boston, MA 02115. E-mail seidman@rascal.med.harvard.edu

© 2003 American Heart Association, Inc.

*Circulation* is available at <http://www.circulationaha.org>

DOI: 10.1161/01.CIR.0000075270.13497.2B

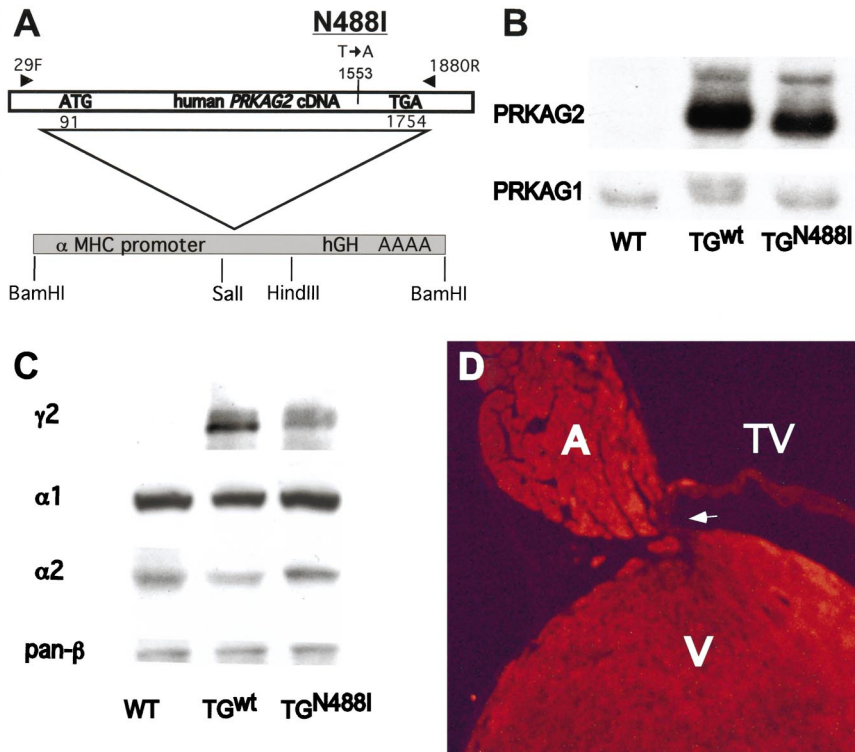


**Figure 1.** PRKAG2 expression in transgenic mice made using a transgene (A) containing either wild-type PRKAG2 cDNA or PRKAG2 cDNA bearing N488I missense mutation (at nucleotide 1553). A, PRKAG2 cDNA was constructed by RT-PCR, using oligonucleotide primers 29F and 1880R, as described (see Methods). Mutant and wild-type PRKAG2 cDNAs were placed under control of  $\alpha$ -MHC promoter. B, Northern blot analyses using PRKAG1 and PRKAG2 cRNA probes to assess expression in nontransgenic wild-type (WT), TG<sup>wt</sup> (line 4657), and TG<sup>N488I</sup> (line 4623) mice. Note that there is more PRKAG2 mRNA than PRKAG1 mRNA in nontransgenic wild-type hearts; PRKAG2 mRNA is detectable in wild-type hearts after longer exposure. C, Western blot analyses using antibodies specific for AMPK subunits ( $\gamma_2$ ,  $\alpha_1$ ,  $\alpha_2$ , and pan- $\beta$ ) reacted with cardiac extracts from WT, TG<sup>wt</sup>, and TG<sup>N488I</sup> mice. AMPK  $\gamma_2$  subunit is 63 kDa, and  $\beta_1$  subunit is 40 kDa. D, Immunofluorescence staining of a TG<sup>N488I</sup> heart section containing right atrium (A), right ventricle (V), tricuspid valve (TV), and annulus fibrosus (arrow) using AMPK  $\gamma_2$  subunit antibody.

patterns of ventricular preexcitation and other features associated with WPW.<sup>2,5,8</sup> WPW is generally thought to be caused by muscular tracts that connect atrium to ventricle outside the specialized conduction tissue such that electrical impulses traversing these tracts bypass the physiological atrioventricular node delay and produce ventricular preexcitation. In most patients with WPW, however, the anatomic substrate for ventricular preexcitation is undefined. Morphological studies of hearts from individuals with PRKAG2 mutations have not been performed, and whether these mutations cause bypass tracts is unknown.

We developed transgenic mice overexpressing the PRKAG2 N488I missense mutation to define the mechanisms by which this mutation causes cardiac disease; because human PRKAG2 mutations create a “gain of function,”<sup>5</sup> a transgenic mouse overexpressing the mutant gene appeared to be a suitable model system. The transgenic mice expressed either wild-type or mutant (N488I) PRKAG2 cDNA under control of the cardiac-specific  $\alpha$ -myosin heavy chain ( $\alpha$ -MHC) promoter<sup>9</sup> (Figure 1A). Transgenic mice carrying the mutant but not wild-type human PRKAG2 cDNA developed both cardiac hypertrophy and ventricular preexcitation. Our analyses of these mice define the anatomic basis for preexcitation in this human cardiomyopathy.

## Methods

### Transgenic Mice

The PRKAG2 coding region was amplified from human lymphocyte RNA by use of the One-Step reverse transcription–polymerase chain reaction (RT-PCR) kit (Qiagen) with primers 29F, 5′-GGGAGGGAAGGAGGGGACCGAACC-3′, and 1880R, 5′-GCAGCCAGTGTTCATGAGGCAAAAC-3′. An 1851-bp fragment was isolated and subcloned into pCR<sup>R</sup>IITOPOR<sup>R</sup> vector (TOPO TA cloning kit, Invitrogen). The nucleotide sequences of 20 cloned

inserts were determined to identify 1 insert that was identical to human PRKAG2 cDNA. A T→A substitution was introduced at nucleotide residue 1553 to encode the Asn→Ile missense mutation (at codon 488, designated N488I<sup>F</sup>). Wild-type and mutant cDNA inserts were released by EcoRI digestion and blunt-end–ligated into the Sall site of pC126 expression vector.<sup>9</sup> Transgene DNA encoding the  $\alpha$ -MHC promoter, PRKAG2 coding sequence, human growth hormone 3′-UTR, and a polyA signal (Figure 1A) were linearized with BamHI; size-fractionated; purified (QIAquick Gel Extraction Kit, Qiagen); and microinjected into fertilized FVB mouse oocytes.

### Genotyping

Transgenic founders were identified by Southern blot analyses of tail DNA as described previously,<sup>10</sup> except that a 540-bp antisense biotinylated riboprobe (Strip-EZ RNA Kit, Ambion) corresponding to the 3′ end of the cloned cDNA was used to identify the 1000-bp HindIII transgene-specific fragment. Offspring of founder mice were genotyped by PCR amplification of the transgene using primers F, 5′-GCCTGCTTTCATGAAGCAGAA-3′, and R, 5′-GCAGCCAGTGTTCATGAGGCAAAAC-3′, and a control mouse genomic fragment using primers F, 5′-GAGAACTCGGCATGCCAGATTC-3′, and R, 5′-ACTCAGCAAGCCTTCCCCTCTG-3′, in 1 reaction.

### RNA Assessment

Northern blots were performed as described<sup>10</sup> using 2  $\mu$ g total cardiac RNA per gel lane and biotinylated riboprobes prepared as above. Semiquantitative RT-PCR using the above-mentioned PRKAG1 and PRKAG2 primers was performed as described.<sup>11</sup> Band intensities were quantified by densitometry using NIH Image software.

### Protein Analyses

Protein extracts and Western blots were performed as described<sup>6</sup> using 10 to 20  $\mu$ g of protein lysate per lane. Antibodies specific for the AMPK  $\gamma_2$  peptide (556 to 569 LTPAGAKQKETETE-COOH),  $\alpha_1$ ,  $\alpha_2$ , and pan- $\beta$  (Upstate Biotechnology) were diluted 1000- to 2000-fold. Horseradish peroxidase–conjugated secondary antibody was used for chemiluminescence detection.

**Characteristics of Wild-Type, TG<sup>wt</sup>, and TG<sup>N488I</sup> Hearts**

Parameter	Strain			P	
	Wild-Type	TG <sup>wt</sup>	TG <sup>N488I</sup>	TG <sup>wt</sup> vs WT	TG <sup>N488I</sup> vs TG <sup>wt</sup>
HW/BW, mg/g	4.8±0.2	7.0±0.4	11.5±1.4	<0.001	<0.001
Water/HW, %	77.0±1.6	74.7±0.7	75.0±1.3	0.03	NS
Protein/HW, %	14.6±5.7	14.7±3.3	15.6±3.8	NS	NS
Glycogen/HW*	1.6±0.7	10.1±1.2	52.9±3.4	<0.001	<0.001
Echocardiography					
8–10 Weeks					
Heart rate, bpm	607±82	549±48	504±62	NS	0.04
LVWT, mm	0.90±0.08	0.99±0.08	1.22±0.23	0.05	0.03
LVEDD, mm	2.42±0.19	2.51±0.49	3.15±0.45	NS	0.03
FS, %	67.2±7.1	75.5±5.7	56.9±9.3	0.03	<0.001
20 Weeks					
Heart rate, bpm	592±96	484±47	475±40	NS	NS
LVWT, mm	0.89±0.11	1.02±0.06	1.25±0.12	NS	0.014
LVEDD, mm	2.49±0.25	2.74±0.50	4.14±0.51	NS	0.008
FS, %	78.1±4.8	76.3±6.2	34.4±7.8	NS	<0.001

HW/BW indicates ratio of wet heart weight to body weight; LVWT, maximum left ventricular wall thickness; LVEDD, left ventricular end-diastolic diameter; and FS, fractional shortening. Data (mean±SD) reflect 4–10 mice evaluated in each group.

\*Micrograms per milligram wet weight.

### Biochemical Assays

Glycogen content was determined by the amyloglucosidase digestion method<sup>12</sup> on cardiac tissue that was rapidly excised, instantly immersed in ice-cold PBS, blotted, and freeze-clamped. Glucose was determined with the glucose oxidase kit (Sigma). AMPK activity was assessed by its ability to phosphorylate a synthetic peptide.<sup>13</sup> AMPK complexes were immunoprecipitated from 200 µg protein using α<sub>1</sub>- or α<sub>2</sub>-specific antibody and protein A/G Plus-Agarose beads (Santa Cruz Biotechnology). AMPK activity with or without 200 µmol/L AMP was determined by the phosphorylation of a synthetic "SAMS" peptide (HMRSAMSGHLVKKR).

### Echocardiography and ECG

Echocardiography was performed in male mice with a SONOS-4500 Hewlett-Packard echocardiograph as described previously,<sup>10</sup> except that mice were anesthetized before hair removal. ECG recordings, electrophysiological studies, and continuous ECG recordings (Holter monitor) were performed as described previously.<sup>14</sup>

### Histopathology

Mouse hearts were fixed and stained as described previously.<sup>5,10</sup> Sections for immunohistochemistry were deparaffinized, incubated with AMP kinase γ<sub>2</sub> antibody and fluorescein-conjugated secondary antibody, and examined under a fluorescence microscope. For electron microscopy, 1-µm sections fixed in glutaraldehyde were embedded in Epon 812 and stained with toluidine blue. Hearts were analyzed for accessory atrioventricular connections by serial analyses of 5-µm sections taken every 20 µm.<sup>15,16</sup> The morphology of the native conduction system was analyzed in genetically engineered mice that express β-galactosidase under the endogenous MinK promoter.<sup>17</sup> β-Galactosidase was assayed in whole explanted hearts by use of an X-gal-based kit from Specialty Media (www.SpecialtyMedia.com).

### Data Analysis

Preliminary studies of TG<sup>wt</sup> lines 4656, 4657, and 4671 and TG<sup>N488I</sup> lines 4623, 4625, 4636, 4645, and 4649 indicated that all lines shared phenotypic features (ie, heart size, glycogen content, histopathology). Lines 4657 and 4623 and control littermates were selected for

detailed analyses (see text). All data are presented as mean±SD and analyzed by Student's *t* test.

## Results

A full-length human *PRKAG2* cDNA, which encodes a 569-amino-acid polypeptide<sup>18</sup> and is 95% similar to the mouse homologue, was amplified from lymphocyte RNA and used as a transgene (see Methods and Figure 1A). A second transgene was created by mutating codon 488 from Asn→Ile. Seven independent transgenic lines expressed robust amounts of wild-type *PRKAG2* RNA (denoted TG<sup>wt</sup>), and 8 independent lines expressed abundant N488I *PRKAG2* RNA (denoted TG<sup>N488I</sup>) levels. Heterozygous offspring from TG<sup>wt</sup> founder 4657 and TG<sup>N488I</sup> founder 4623 were used for further analyses because of comparable transgene RNA expression. Each transgenic mouse carried ≈20 copies of the transgene (data not shown) and expressed at least 20-fold more cardiac *PRKAG2* RNA than nontransgenic mice (Figure 1B).

Transgene-encoded AMPK γ<sub>2</sub> protein was not detected in newborn transgenic mice, presumably because the α-MHC promoter does not become fully active until after neonatal life.<sup>19</sup> In young and adult transgenic mice, AMPK γ<sub>2</sub> protein was abundant in atrial and ventricular myocardium (Figure 1, C and D). AMPK γ<sub>2</sub> protein levels in TG<sup>N488I</sup> and TG<sup>wt</sup> hearts were ≈20-fold higher than endogenous γ<sub>2</sub> subunit protein levels in nontransgenic mice, but *PRKAG2* overexpression did not affect the levels of endogenous *PRKAG1* mRNA or the levels of other AMPK subunits (Figure 1, B and C).

Transgenic *PRKAG2* mice were viable and fertile. TG<sup>wt</sup> and TG<sup>N488I</sup> mice had significant increases in cardiac glycogen (Table) compared with levels found in nontransgenic controls, but cardiac glycogen was markedly greater in TG<sup>N488I</sup> than TG<sup>wt</sup> mice. Cardiac anatomy of TG<sup>wt</sup> mice showed only

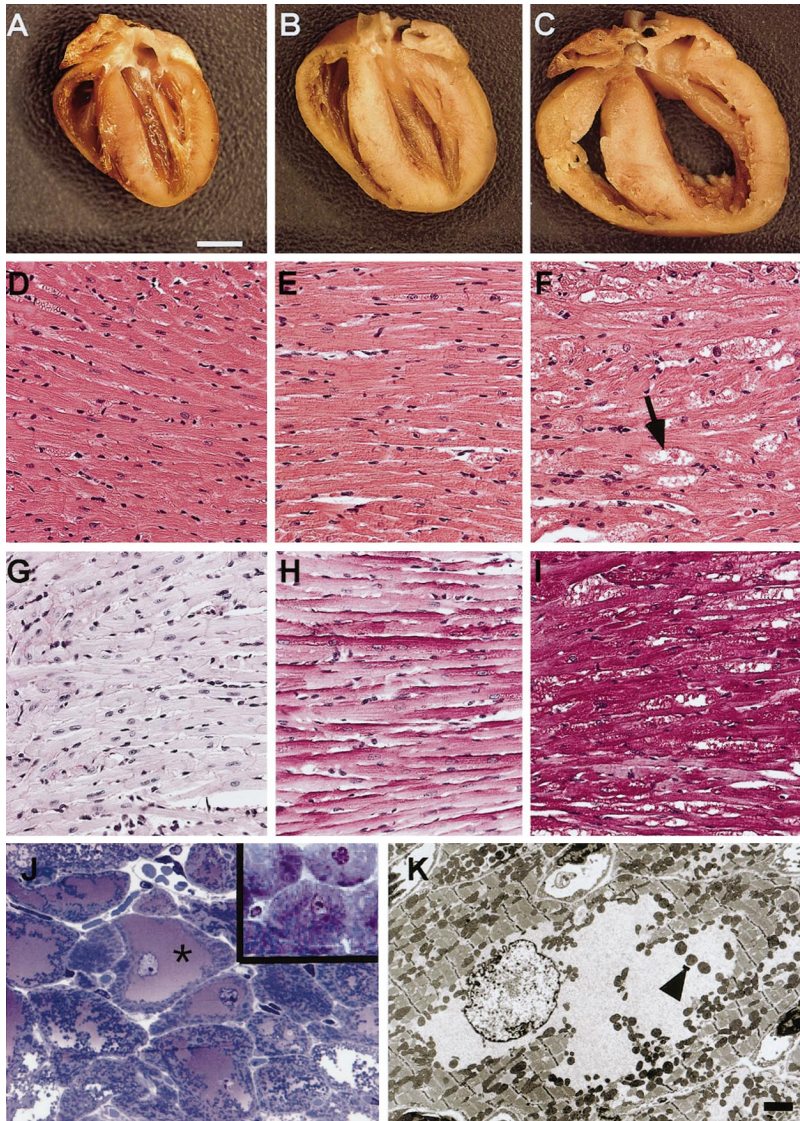


**Figure 2.** Cardiac morphology and histology of 8-week-old mice. Longitudinal sections from wild-type (A), TG<sup>wt</sup> (B), and TG<sup>N488I</sup> (C) hearts demonstrate cardiac hypertrophy in *PRKAG2* transgenic mice (bar=2 mm). Sections from wild-type (D), TG<sup>wt</sup> (E), and TG<sup>N488I</sup> (F) hearts stained with hematoxylin and eosin. Note markedly distended myocytes with vacuolated cytoplasm (arrow) in TG<sup>N488I</sup> samples (magnification 400 $\times$ ). PAS-stained sections from wild-type (G), TG<sup>wt</sup> (H), and TG<sup>N488I</sup> (I) hearts (400 $\times$ ). Sections stained with PAS followed by diastase digestion were negative (data not shown). J, TG<sup>N488I</sup> heart section stained with toluidine blue revealed markedly distended myocytes filled with glycogen (homogeneous purple pools). Inset shows granular appearance of organelles and cytoplasm from a wild-type heart. K, Electron micrograph of a hypertrophied TG<sup>N488I</sup> myocyte shows abundant non-membrane-bound glycogen (pale, fine-grained material), displaced mitochondria (arrowhead), and peripheral myofibrils (uranyl acetate and lead citrate; bar=3  $\mu$ m).

mild morphological changes despite significantly increased glycogen content. Cardiac weight and left ventricular wall thickness were increased compared with wild-type mouse hearts (Table), but TG<sup>wt</sup> hearts had neither histopathological changes (Figure 2) nor cardiac dysfunction associated with glycogen storage. In contrast, TG<sup>N488I</sup> mice had strikingly abnormal cardiac morphology and histology. Cardiac mass and left ventricular wall thickness were markedly increased in TG<sup>N488I</sup> mice compared with nontransgenic controls or TG<sup>wt</sup> mice (Figure 2, A–C, and Table). Histological analyses (Figure 2, D–I) showed myocyte hypertrophy; PAS staining revealed abundant glycogen throughout the myocardium. Ventricular but not atrial myocytes contained vacuoles, which were similar to those observed in cardiac histopathology of humans bearing a *PRKAG2* mutation.<sup>5</sup> Electron microscopy revealed that vacuoles contained pooled, non-membrane-bound glycogen, which displaced contractile elements and distorted the overall cell morphology (Figure 2K). Neither interstitial fibrosis nor lipid deposition was evident.

The cardiac function of TG<sup>N488I</sup> mice deteriorated over time. Echocardiograms of TG<sup>N488I</sup> mice showed cardiac hy-

pertrophy with near-normal fractional shortening at 8 to 10 weeks, but by 20 weeks of age, contractile function was reduced and chamber dilation was evident (Table). Cardiac hypertrophy was associated with a proportional increase in protein content (Table) and augmented ventricular expression of hypertrophy-related genes: atrial natriuretic peptide (ANP), brain natriuretic peptide (BNP), and  $\alpha$ -skeletal actin (Figure 3). ANP, BNP, and  $\alpha$ -skeletal actin RNA in TG<sup>wt</sup> hearts were 6-, 3-, and 4-fold greater than in nontransgenic hearts, respectively (3 to 4 mice per group;  $P<0.05$ ), whereas these RNAs were 20-, 10-, and 8-fold greater in TG<sup>N488I</sup> than in nontransgenic hearts. ANP and BNP RNAs were expressed at a significantly higher level in TG<sup>N488I</sup> than in TG<sup>wt</sup> hearts ( $P<0.025$ ).

Because human *PRKAG2* missense mutations caused ventricular preexcitation and progressive conduction system disease,<sup>2,5,8,20</sup> cardiac electrophysiology was studied in transgenic mice. Surface ECGs (Figure 4A) showed that  $\approx 50\%$  of TG<sup>N488I</sup> mice had shortened PR intervals, indicative of a reduction in the physiological time delay between atrial and ventricular electrical activation, and delta waves, suggestive

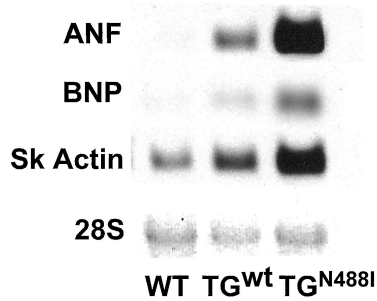


**Figure 3.** Expression of hypertrophy-associated genes in cardiac ventricles of 8-week-old wild-type (WT) and transgenic (TG<sup>wt</sup> and TG<sup>N488I</sup>) animals. Northern blots were probed with ANP (ANF), BNP, and  $\alpha$ -skeletal actin (Sk actin) cRNA probes.

of ventricular preexcitation. Concurrent ECGs and 2D echocardiography indicated that preexcitation was associated with asynchronous left ventricular contraction. Preexcitation was not found in any TG<sup>wt</sup> mice ( $n=18$ ) or in  $>200$  wild-type mice.

Invasive electrophysiological studies (Figure 4B) confirmed preexcitation in 2 independent TG<sup>N488I</sup> lines. Two distinct pathways for atrioventricular conduction were observed with different coupling intervals and different ventricular morphologies of excitation (our unpublished results). Continuous ECG recordings showed that multiple patterns of ventricular activation coexisted in the same animal (Figure

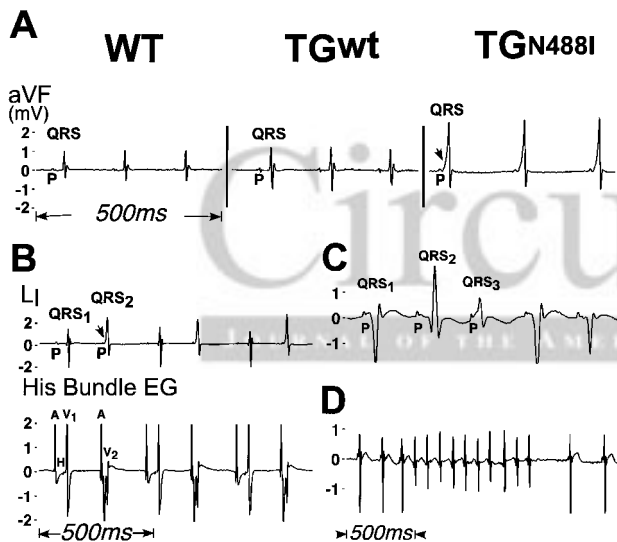


**Figure 4.** Electrophysiological analyses of wild-type (WT) and transgenic (TG<sup>wt</sup> and TG<sup>N488I</sup>) animals. A, Surface ECG (aVF lead) from wild-type (WT), TG<sup>wt</sup>, and TG<sup>N488I</sup> mice. Note short PR interval and delta wave (arrow) in traces from TG<sup>N488I</sup> mice. B, Surface L<sub>1</sub> lead (top) and His-bundle electrogram (bottom) from a TG<sup>N488I</sup> mouse demonstrates physiological conduction, revealed by sequential atrial (A), His bundle (H), and ventricular (V<sub>1</sub>) activation and preexcitation (A, V<sub>2</sub> in absence of His-bundle potential). Note distinct QRS morphologies with physiological conduction vs preexcitation. C, Holter recording of TG<sup>N488I</sup> mice showing sinus rhythm and preexcitation with variable QRS morphologies (QRS<sub>1</sub>, QRS<sub>3</sub>) suggestive of multiple accessory atrioventricular connections. QRS<sub>2</sub> is a nonpreexcited beat. D, Paroxysmal supraventricular tachycardia and sinus bradycardia recorded from a TG<sup>N488I</sup> mouse.

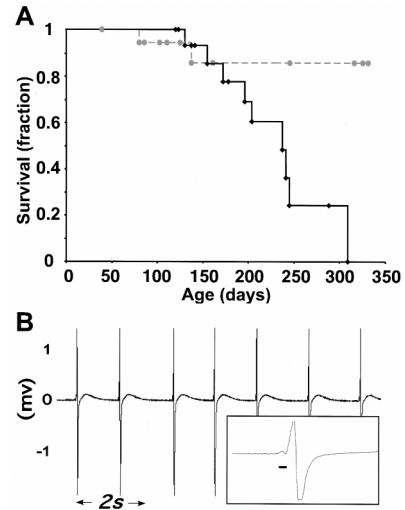


**Figure 5.** Early mortality and preterminal heart rhythm observed in TG<sup>N488I</sup> mice. A, Kaplan-Meier survival curves of (diamonds) TG<sup>N488I</sup> and (circles) TG<sup>wt</sup> mice. B, Holter monitor tracing from a 44-week-old TG<sup>N488I</sup> mouse, taken shortly before death, shows a severe bradycardia (heart rate of this TG<sup>N488I</sup> mouse was  $<60$  bpm, whereas normal mouse heart rate is  $>400$  bpm). Note that PR interval remains short (normal  $\approx 30$  ms). Inset shows a magnified P-QRS complex (bar=20 ms).

4C), analogous to electrophysiological observations in human patients with *PRKAG2* mutations and WPW.<sup>8</sup>

TG<sup>N488I</sup> mice had a lower basal heart rate (Table), and on continuous ECG monitoring ( $n=6$ ), all exhibited deterioration of the conduction system with frequent spontaneous episodes of sinus bradycardia ( $<300$  bpm) and various escape rhythms, including paroxysmal supraventricular tachycardia and atrial fibrillation (Figure 4D). Stress (induction of anesthesia and/or manipulation) resulted in syncope and led to sudden death in 5 TG<sup>N488I</sup> mice; ECG monitoring of stressed TG<sup>N488I</sup> mice suggested severe and persistent sinus bradycardia as the cause of death. Spontaneous mortality, associated with severe left ventricular dysfunction, was observed in TG<sup>N488I</sup> mice 20 to 40 weeks old (Figure 5A). Continuous ECG recording in 3 old mice ( $>30$  weeks old) (Figure 5B) demonstrated severe sinus bradycardia but not tachyarrhythmia or atrioventricular block before death.

To examine the specialized cells of the conduction system, TG<sup>N488I</sup> mice were crossed with minK-LacZ mice,<sup>17</sup> which transcribe  $\beta$ -galactosidase mRNA under control of the minK promoter so that  $\beta$ -galactosidase was expressed in cardiac conduction system cells. Compound mutant mice (MinK/TG<sup>N488I</sup>) had no evidence of gross abnormalities in the cardiac conduction system compared with wild-type MinK mice (data not shown). Although the gross organization of the conduction system was normal, serial histological examination of the atrioventricular junction in TG<sup>N488I</sup> mice showed important differences (Figure 6). The annulus fibrosus, which normally insulates the atria from the ventricles, was a continuous structure in both wild-type and TG<sup>wt</sup> hearts. However, in hypertrophied TG<sup>N488I</sup> hearts, the annulus fibrosus was thinned, stretched, and disrupted, most notably at the atrioventricular junction above the interventricular septum. This region contained many vacuolated, glycogen-loaded

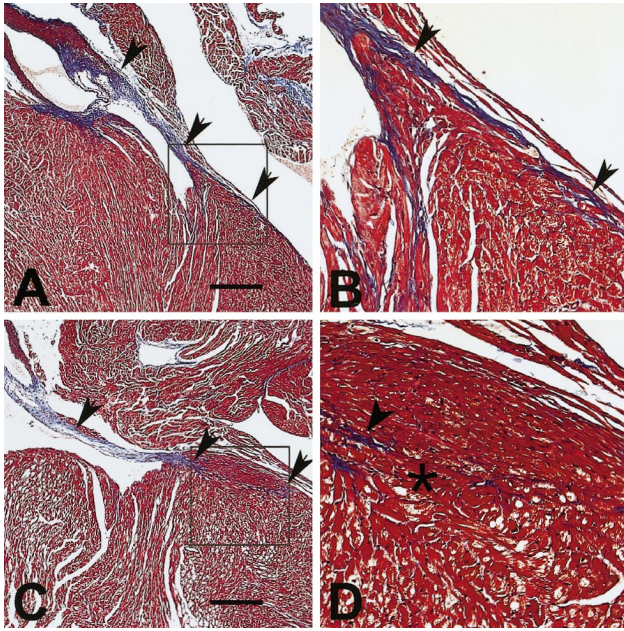


**Figure 6.** Masson's trichrome–stained sections from TG<sup>wt</sup> (A, B) and TG<sup>N488I</sup> (C, D) myocardium including right paraseptal area, lateral to aortic outflow tract. A, C, Sections were examined with a low-power objective lens (bar=200  $\mu$ m). Blue-staining annulus fibrosis (arrows), fibrous separation between atria and ventricles, is intact in TG<sup>wt</sup> (A) but disrupted in TG<sup>N488I</sup> (C) hearts. Boxed regions (A, C) examined at higher magnification (4 $\times$ ) demonstrate intact annulus fibrosis in TG<sup>wt</sup> hearts (B) and discontinuous annulus fibrosis in TG<sup>N488I</sup> hearts (D). Note physical contact (\*) between atrial and vacuolated ventricular myocytes in TG<sup>N488I</sup> heart.

myocytes. However, all TG<sup>N488I</sup> hearts studied (n=5) showed loss of fibrous separation between atrial and ventricular myocardium in the anterior septum lateral to the aortic outflow tract and adjacent to the tricuspid annulus (the region defined by surface ECG criteria as the locus of preexcitation). Furthermore, 2 TG<sup>N488I</sup> hearts also showed disruption of annulus fibrosis in the posterior septal region, consistent with multiple accessory AV connections, as suggested by continuous ECG monitoring (Figure 4C). No distinct bypass tracts were observed.

AMPK activity, with and without AMP stimulation, was measured in cardiac extracts from young TG<sup>wt</sup> and TG<sup>N488I</sup> mice after immunoprecipitation with  $\alpha$ -subunit–specific antibodies (Figure 7). AMP stimulation produced a modest (<2-fold) increase in  $\alpha_1$  or  $\alpha_2$  subunit–associated AMPK activity in wild-type or transgenic heart extracts. Both  $\alpha_1$  and  $\alpha_2$  subunit–associated basal AMPK activity was increased in TG<sup>N488I</sup> mice compared with TG<sup>wt</sup> mice. In TG<sup>N488I</sup> hearts, AMPK activity associated with the  $\alpha_2$  subunit demonstrated a much more dramatic increase ( $\approx$ 8-fold versus <2-fold) than the increase in  $\alpha_1$  subunit–associated AMPK activity in these same mice (Figure 7).

## Discussion

We demonstrate that transgenic mice overexpressing mutant PRKAG2 exhibit the cardiomyopathy and electrophysiological abnormalities found in humans with this mutation.<sup>2–5</sup> Transgenic mice expressing mutant PRKAG2 demonstrated

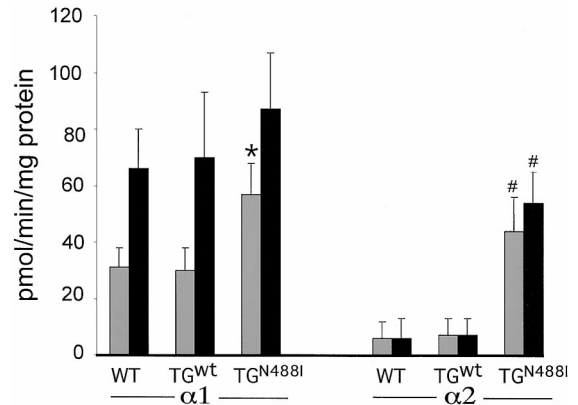


**Figure 7.** AMPK activity in nontransgenic wild-type (WT) and transgenic mouse hearts. Non-AMP–stimulated (basal, gray bars) and AMP–stimulated (black bars) AMPK activity in cardiac extracts of 1-week-old WT, TG<sup>wt</sup>, and TG<sup>N488I</sup> mice (n=3 to 4 per group). AMPK activity was measured after immunoprecipitation with antibodies specific for  $\alpha_1$  or  $\alpha_2$ . TG<sup>N488I</sup> extracts had significantly more basal  $\alpha_1$ -subunit–associated AMPK and  $\alpha_2$ -subunit associated AMPK activity than TG<sup>wt</sup> or wild-type hearts (\* $P$ <0.02, # $P$ <0.002).

increased cardiac enzyme activity and cardiac glycogen storage. In contrast, overexpression of wild-type PRKAG2 produced only mild glycogen accumulation, mild cardiac hypertrophy, and no conduction system disease. These data establish PRKAG2 mutations as a glycogen storage cardiomyopathy and confirm for the first time the direct relationship between PRKAG2 mutations, AMPK activation, glycogen storage, and the features of human disease. Analyses of the atrioventricular junction of these mice explain the preexcitation found in mice and presumably humans with these mutations.

Increased cardiac expression of either wild-type or mutant PRKAG2 cDNA led to increased glycogen storage. Pharmacological activation of AMPK has previously been shown to increase glycogen.<sup>21,22</sup> Intermediate glycogen levels observed in TG<sup>wt</sup> mice were presumably a result of a small, undetectable increase in AMPK activity (Figure 7).<sup>6,23</sup> By age 5 weeks, TG<sup>N488I</sup> hearts contained  $\approx$ 5-fold more glycogen than TG<sup>wt</sup> hearts and 30-fold more glycogen than nontransgenic wild-type hearts, consistent with the significant increases in AMPK activity detected in the transgenic animals (Figure 7).

Comparison of the pathophysiology of PRKAG2 mutations with other glycogen storage diseases provides useful clues to the mechanism of cardiomyopathy and conduction system disease. Cardiac hypertrophy is a common feature of several other inherited disorders of glycogen metabolism.<sup>24–26</sup> Mice lacking the  $\alpha$ -glucosidase gene, a model of Pompe's disease, show progressive accumulation of glycogen (up to 140  $\mu$ g/mg protein) and cardiac hypertrophy,<sup>12,27</sup> quite like TG<sup>N488I</sup> mice, thereby supporting the concept that glycogen accumulation per se accounts for cardiac hypertrophy.

Many glycogen storage disorders also cause conduction system disease, and some have ECG patterns suggestive of preexcitation. Although an ECG pattern of WPW is sometimes found in Pompe disease,<sup>15,25</sup> it is more frequently observed with Danon disease, a cardiac and skeletal myop-

athy with encephalopathy, preexcitation, and bradyarrhythmias.<sup>26</sup> Because no histologically defined bypass tracts have been identified, these individuals are often presumed to have accelerated AV nodal conduction or abnormal fasciculoventricular connections.<sup>15,16,20</sup> Disruption of annulus fibrosis has also been identified in some patients with WPW<sup>28,29</sup> unassociated with glycogen storage disease. We suggest that disruption of the annulus fibrosis by glycogen-filled myocytes, rather than distinct bypass tracts, is the likely mechanism for preexcitation in these diseases. Distinguishing between WPW caused by muscular bypass tracts rather than disruption of the annulus fibrosis may have clinical significance, particularly with regard to ablation therapies.

Our studies also suggest an explanation for the cardiac conduction defects caused by glycogen accumulation.<sup>2,5,15,24,26</sup> Glycogen accumulation after conduction system development is complete leads to remodeling of atrioventricular conduction pathways in TG<sup>N4881</sup> mice. Whether glycogen accumulation in humans bearing these mutations occurs during or after conduction system development is unclear. Perhaps postnatal reversal of glycogen accumulation will restore normal cardiac conduction. Analyses of transgenic mice bearing mutant *PRKAG2* whose expression can be controlled will answer this question.

### Acknowledgments

This work was supported by the Howard Hughes Medical Institute (M.A., C.E.S., J.G.S.), the NHMRC Australia (D.S.) and National Institutes of Health grant HL-46681 (D.M.R.). We thank Dr Jeffrey Robbins for the generous gift of the  $\alpha$ -MHC promoter vector and Dr David Conner for helpful advice.

### References

- Kemp BE, Mitchelhill KI, Stapleton D, et al. Dealing with energy demand: the AMP-activated protein kinase. *Trends Biochem Sci.* 1999; 24:22–25.
- Gollob MH, Green MS, Tang AS, et al. Identification of a gene responsible for familial Wolff-Parkinson-White syndrome. *N Engl J Med.* 2001;344:1823–1831.
- Blair E, Redwood C, Ashrafian H, et al. Mutations in the gamma (2) subunit of AMP-activated protein kinase cause familial hypertrophic cardiomyopathy: evidence for the central role of energy compromise in disease pathogenesis. *Hum Mol Genet.* 2001;10:1215–1220.
- Gollob MH, Seger JJ, Gollob TN, et al. Novel *PRKAG2* mutation responsible for the genetic syndrome of ventricular preexcitation and conduction system disease with childhood onset and absence of cardiac hypertrophy. *Circulation.* 2001;104:3030–3033.
- Arad M, Benson DW, Perez-Atayde AR, et al. Constitutively active AMP kinase mutations cause glycogen storage disease mimicking hypertrophic cardiomyopathy. *J Clin Invest.* 2002;109:357–362.
- Hamilton SR, Stapleton D, O'Donnell JB Jr, et al. An activating mutation in the gamma1 subunit of the AMP-activated protein kinase. *FEBS Lett.* 2001;500:163–168.
- Arad M, Seidman JG, Seidman CE. Phenotypic diversity in hypertrophic cardiomyopathy. *Hum Mol Genet.* 2002;11:2499–2506.
- Mehdirad AA, Fatkin D, DiMarco JP, et al. Electrophysiologic characteristics of accessory atrioventricular connections in an inherited form of Wolff-Parkinson-White syndrome. *J Cardiovasc Electrophysiol.* 1999; 10:629–635.
- Subramaniam A, Jones WK, Gulick J, et al. Tissue-specific regulation of the alpha-myosin heavy chain gene promoter in transgenic mice. *J Biol Chem.* 1991;266:24613–24620.
- Semsarian C, Ahmad I, Giewat M, et al. The L-type calcium channel inhibitor diltiazem prevents cardiomyopathy in a mouse model. *J Clin Invest.* 2002;109:1013–1020.
- Rajeevan MS, Ranamukhaarachchi DG, Vernon SD, et al. Use of real-time quantitative PCR to validate the results of cDNA array and differential display PCR technologies. *Methods.* 2001;25:443–451.
- Raben N, Danon M, Lu N, et al. Surprises of genetic engineering: a possible model of polyglucosan body disease. *Neurology.* 2001;56: 1739–1745.
- Hardie DG, Salt IP, Davies SP. Analysis of the role of AMP-activated protein kinase in the response to cellular stress. In: S.M. Keyse, ed. *Stress Response, Methods and Protocols.* Totowa, NJ: Humana Press; 2001: 63–74.
- Berul CI, McConnell BK, Wakimoto H, et al. Ventricular arrhythmia vulnerability in cardiomyopathic mice with homozygous mutant myosin-binding protein C gene. *Circulation.* 2001;104:2734–2739.
- Bulkeley BH, Hutchins GM. Pompe's disease presenting as hypertrophic myocardiopathy with Wolff-Parkinson-White syndrome. *Am Heart J.* 1978;96:246–252.
- Bharati S, Serratto M, DuBrow I, et al. The conduction system in Pompe's disease. *Pediatr Cardiol.* 1982;2:25–32.
- Kupersmidt S, Yang T, Anderson ME, et al. Replacement by homologous recombination of the minK gene with lacZ reveals restriction of minK expression to the mouse cardiac conduction system. *Circ Res.* 1999;84:146–152.
- Cheung PC, Salt IP, Davies SP, et al. Characterization of AMP-activated protein kinase gamma-subunit isoforms and their role in AMP binding. *Biochem J.* 2000;346(pt 3):659–669.
- Reiss K, Cheng W, Ferber A, et al. Overexpression of insulin-like growth factor-1 in the heart is coupled with myocyte proliferation in transgenic mice. *Proc Natl Acad Sci U S A.* 1996;93:8630–8635.
- Gollob MH, Green MS, Tang AS, et al. *PRKAG2* cardiac syndrome: familial ventricular pre-excitation, conduction system disease, and cardiac hypertrophy. *Curr Opin Cardiol.* 2002;17:229–234.
- Holmes BF, Kurth-Kraczek EJ, Winder WW. Chronic activation of 5'-AMP-activated protein kinase increases GLUT-4, hexokinase, and glycogen in muscle. *J Appl Physiol.* 1999;87:1990–1995.
- Aschenbach WG, Hirshman MF, Fujii N, et al. Effect of AICAR treatment on glycogen metabolism in skeletal muscle. *Diabetes.* 2002;51: 567–573.
- Milan D, Jeon JT, Looft C, et al. A mutation in *PRKAG3* associated with excess glycogen content in pig skeletal muscle. *Science.* 2000;288: 1248–1251.
- Verloes A, Massin M, Lombet J, et al. Nosology of lysosomal glycogen storage diseases without in vitro acid maltase deficiency: delineation of a neonatal form. *Am J Med Genet.* 1997;72:135–142.
- Francesconi M, Auff E. Cardiac arrhythmias and the adult form of type II glycogenosis. *N Engl J Med.* 1982;306:937–938.
- Sugie K, Yamamoto A, Murayama K, et al. Clinicopathological features of genetically confirmed Danon disease. *Neurology.* 2002;58:1773–1778.
- Bijvoet AG, van de Kamp EH, Kroos MA, et al. Generalized glycogen storage and cardiomegaly in a knockout model of Pompe disease. *Hum Mol Genet.* 1998;7:53–62.
- Basso C, Corrado D, Rossi L, et al. Ventricular preexcitation in children and young adults. *Circulation.* 2001;103:269–275.
- Keller BB, Mehta AV, Shamszadeh, et al. Oncocytic cardiomyopathy of infancy with Wolff-Parkinson-White syndrome and ectopic foci causing tachydyrhythmias in children. *Am Heart J.* 1987;144:782–792.